Macromolecules
ARTICLE

Macromolecules **2009**, *42*, 5933–5940 **5933**
DOI: 10.1021/ma9010389

Design and Synthesis of Charge-Transfer-Based Conjugated Polyelectrolytes as Multicolor Light-Up Probes

Kan-Yi Pu, Liping Cai, and Bin Liu*

Department of Chemical and Biomolecular Engineering, 4 Engineering Drive 4, National University of Singapore, Singapore 117576

Received May 13, 2009; Revised Manuscript Received July 1, 2009

ABSTRACT: Cationic poly[9,9-bis(6′-*N*,*N*,*N*-trimethylammonium)hexyl)fluorene-*alt*-4,7-(2,1,3-benzothiadiazole) dibromide] (PFBT) and poly[9,9-bis(6′-(*N*,*N*,*N*-trimethylammonium)hexyl)fluorenyldivinylene-*alt*-4,7-(2,1,3-benzothiadiazole) dibromide] (PFVBT) are designed and synthesized to serve as multicolor light-up probes for biomolecular quantification. Because of the charge-transfer electronic states of the polymers, they exhibit weak fluorescence in aqueous media which can be significantly enhanced by increasing the hydrophobicity of polymeric microenvironment. Molecular orbital simulations further reveal that the presence of vinyl bonds endows PFVBT with a stronger charge-transfer character relative to that of PFBT. Both PFBT and PFVBT exhibit linear fluorescence enhancement as a function of bovine serum albumin (BSA) or DNA concentration in buffer solution, allowing effective biomolecular quantification. Of particular interest is that the light-up responses of PFBT or PFVBT in the presence of BSA and DNA are different, featuring biomolecule-dependent yellow-to-golden and orange-to-red light-up signatures, respectively. With a more sensitive light-up response, PFVBT can quantify biomolecules more effectively than PFBT does, which highlights the crucial role of charge transfer in determining the microenvironment-responsive fluorescence of conjugated polyelectrolytes for chemical and biological sensing.

Introduction

Molecular recognition and quantification of biological substances are of scientific importance and economic interest in view of their vital applications in pharmaceutics, clinical diagnosis, forensic analysis, and antiterrorism.[1] During the past decades, fluorescent probes have been proven powerful markers in genomics and proteomics.[2] Superior to probes with fluorescence quenching as signal readout, light-up probes with fluorescence turn-on response possess reduced false-positive signal and increased sensitivity, offering a dark background for easy and accurate measurement of trace analytes.[3] The current light-up fluorophores are rare, which often have the drawbacks such as weak light-up contrast, small Stokes shift, nonlinear calibration curve, poor environmental stability, or insufficient water solubility.[4] Development of high-performance light-up probes continues to be an active focus of chemistry, biology, and materials science. A recent advance in this regard is the creation of fluorophores with aggregation-induced emission (AIE), which show fluorescent increases in response to a variety of biomolecules, including proteins, oligonucleotides, and phosphates.[5] Despite their light-up response to different species, the emission maxima of AIE-based fluorophores in the presence of different biomolecules are nearly the same. To ultimately realize naked-eye visualization and cursory recognition of biomolecules, multicolor light-up fluorophores that can generate distinguishable fluorescent colors toward different analytes are in urgent demand.

Conjugated polyelectrolytes (CPEs) are rigid-rod macromolecules with π-conjugated backbones and water-soluble side chains, which integrate optoelectronic properties of conjugated polymers with electrostatic behaviors of polyelectrolytes for construction of chemical and biological probes.[6] The electron-delocalized backbones of CPEs facilitate rapid intrachain and interchain exciton migration, imparting collective optical responses and amplified signals as compared to small molecule fluorophores.[7] To date, most CPEs have been used as fluorescent quenching probes to detect analytes of interest via electron/energy transfer mechanisms or analyte-induced polymer aggregation.[8] Others serve as energy donors to amplify the signal output of dye-labeled biomolecules via Förster resonance energy transfer (FRET).[9] However, CPEs that can inherently generate light-up signatures toward biomolecules are few.[10] By virtue of their light-harvesting properties and structural diversity, CPEs hold great promise in developing multicolor light-up probes.

Electrostatic and hydrophobic interactions play an indispensable role in bringing charged CPEs and biomolecules into close proximity for energy/electron transfer.[11] Polymer aggregation usually concurs with CPE/biomolecule complexation,[12] resulting in three-dimensional interchain exciton migration that is more efficient than one-dimensional intrachain exciton migration due to enhanced electronic coupling.[13] Variations in the optical properties of CPEs upon complexation and the principle of aggregation-enhanced exciton migration have inspired us to design CPE-based probes with energy donor−acceptor architectures for multicolor sensing of biomolecules, such as DNA,[14] heparin,[15] and proteins.[16] Recently, we also reported an intercalating dye harnessed CPE that allowed discrimination of double-strand DNA (dsDNA) from single-strand DNA (ssDNA) in biological media.[17]

Fluorescence principles elucidate that fluorophores with intramolecular charge-transfer electronic states are sensitive to variations in the external environment, and their quantum yields increase as the environment becomes more hydrophobic, ultimately giving rise to dramatic fluorescent responses.[18] Since hydrophobicity apart from water solubility is another important character for biomolecules,[19] the microenvironmental polarity of

*Corresponding author. E-mail: cheliub@nus.edu.sg.

Published on Web 07/10/2009

Scheme 1. Chemical Structures of PFBT and PFVBT

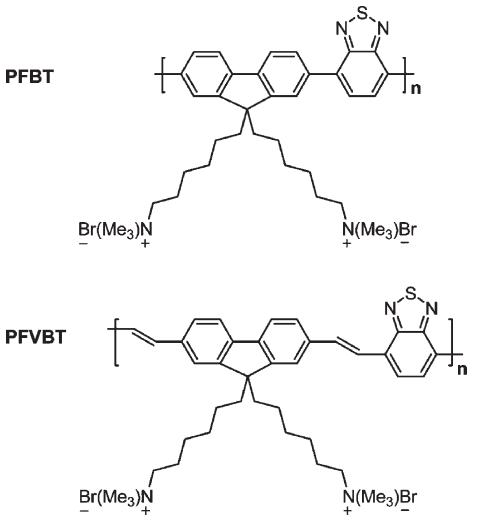

CPEs in aqueous solution is reduced through complexation with biomolecules.[20] In addition, complexation-impelled polymer aggregation also lowers the microenvironmental polarity of CPEs. The complexation-mediated polymeric microenvironment change implicates that it is feasible to develop multicolor light-up probes by incorporating intramolecular charge-transfer character into CPEs.

In this contribution, we report two charge-transfer-based CPEs as multicolor light-up probes for biomolecular quantification. The CPEs are poly[9,9-bis(6′-*N*,*N*,*N*-trimethylammonium)hexyl)fluorene-*alt*-4,7-(2,1,3-benzothiadiazole) dibromide] (PFBT) and poly[9,9-bis(6′-(*N*,*N*,*N*-trimethylammonium)hexyl)-fluorenyldivinylene-*alt*-4,7-(2,1,3-benzothiadiazole) dibromide] (PFVBT) (Scheme 1). The vinyl bonds between fluorene segments and BT units within PFVBT are designed to red-shift the fluorescence as well as to further improve the intramolecular charge-transfer property relative to that of PFBT. The optical properties and charge-transfer electronic states of PFBT and PFVBT are investigated and compared through both spectroscopy studies and molecular orbital simulations. The light-up responses and fluorescent colors of PFBT and PFVBT toward bovine serum albumin (BSA) and DNA are probed in buffer solution. At last, we demonstrate the quantification of BSA and DNA using both polymers.

Results and Discussion

Synthesis and Characterization. Postpolymerization was used to synthesize PFBT as descried in our previous report.[21] After Suzuki coupling polymerization, the resulted neutral precursor was quaternized by trimethylamine to yield PFBT. The number-average degree of polymerization (DP) of PFBT is ~16. On the other hand, Heck coupling polymerization was adopted to incorporate double bonds into the backbone of PFVBT. The reaction medium for Heck polymerization generally involves a basic organic solvent, such as diisopropylamine or triethylamine (TEA). Because of the high reaction temperature (100 °C) in Heck polymerization, monomers with alkyl bromides are likely to react with the basic organic solvent, leading to insoluble byproducts. Therefore, a one-pot polymerization strategy was conducted to directly synthesize PFVBT starting from a quaternary ammonium monomer.

The synthetic route toward PFVBT is shown in Scheme 2. The neutral divinyl monomer, 9,9-bis(6′-bromohexyl)-2,7-divinylfluorene (**2**), was synthesized in 78% yield by heating

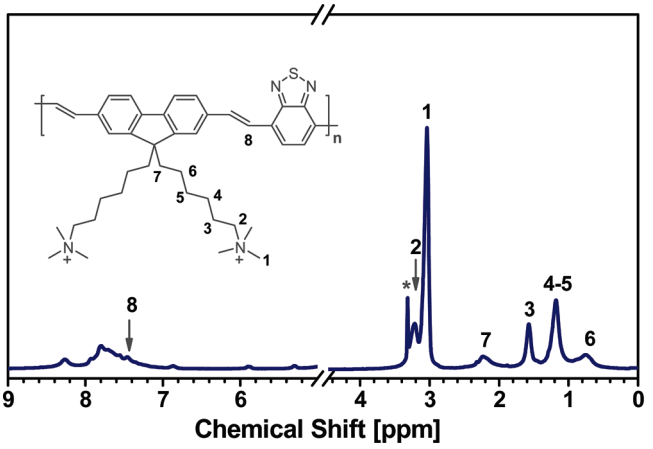

Figure 1. ^{1}H NMR spectrum of PFVBT in CD_3OD. Asterisk indicates the solvent peak. The spectrum is broken to eliminate the strong peak of water at 4.87 ppm.

the mixture of 2,7-dibromo-9,9-bis(6-bromohexyl)fluorene (**1**) and tributylvinyltin in toluene using $PdCl_2(PPh_3)_2$/2,6-di-*tert*-butylphenol as catalyst at 100 °C for 24 h. The correct chemical structure of **2** was proven by NMR and mass spectra as well as elemental analysis. Quaternization of **2** with trimethylamine in THF/H_2O afforded the cationic divinyl monomer, 9,9-bis(6′-(*N*,*N*,*N*-trimethylammonium)-hexyl)-2,7-divinylfluorene dibromide (**3**), in 95% yield. Finally, the water-soluble divinyl monomer **3** was copolymerized with 4,7-dibromobenzothiadiazole (**4**) via a $Pd(OAc)_2$/$P(o\text{-tolyl})_3$-catalyzed Heck coupling reaction in the mixture of DMF/H_2O/TEA (2:1:2) at 100 °C to directly afford the water-soluble cationic polymer PFVBT. This polymer was purified by microfiltration, precipitation, and finally dialysis against Mill-Q water using a 6.5 kDa molecular weight cutoff dialysis membrane for 5 days. The limit of water solubility for PFVBT is ~3 mg/mL, which is slightly better than that of PFBT (~1 mg/mL).

The chemical structure of PFVBT was determined by ^{1}H and ^{13}C NMR spectra. As shown in Figure 1, the absence of resonance peak at ~6.5 ppm illustrates that PFVBT does not have *cis* vinyl protons.[22] The resonance peak of *trans* vinyl protons at ~7.4 ppm is present and mixed with those of aryl protons, giving rise to a broad peak with the maximum at 7.78 ppm. The ratio of the integrated area of the multiple peaks ranging from 8.17 to 7.05 ppm (corresponding to the aryl and vinyl protons) to that of the peak at 2.25 ppm (corresponding to the alkyl protons next to the 9-position of fluorene units) is nearly ~3, which is consistent with the chemical structure of PFVBT. In addition, the weak peaks at 6.91, 5.95, and 5.35 ppm are ascribed to the resonance of vinyl protons of fluorenylvinylene end groups of PFVBT. Comparison of the integrated areas between the peak at 5.95 ppm and the peak at 2.25 ppm reveals that the number-average DP of PFVBT is ~15. These NMR data not only indicate the correct chemical structure of PFVBT but also clarify that PFVBT has a *trans*-CH=CH configuration, which is in accordance with the previous studies of Heck polymerization.[23] The *trans* configuration of PFVBT is beneficial to biosensor application because it facilitates backbone planarization and electron delocalization along the backbone, bringing in a red-shifted absorption and emission spectra as compared to its *cis* counterpart.[24]

Optical Properties. The optical properties of PFVBT and PFBT in solution and solid states are studied and compared. Figure 2 shows the UV−vis absorption and photoluminescence (PL) spectra of PFVBT and PFBT in water. The

Scheme 2. Synthesis of PFVBT[a]

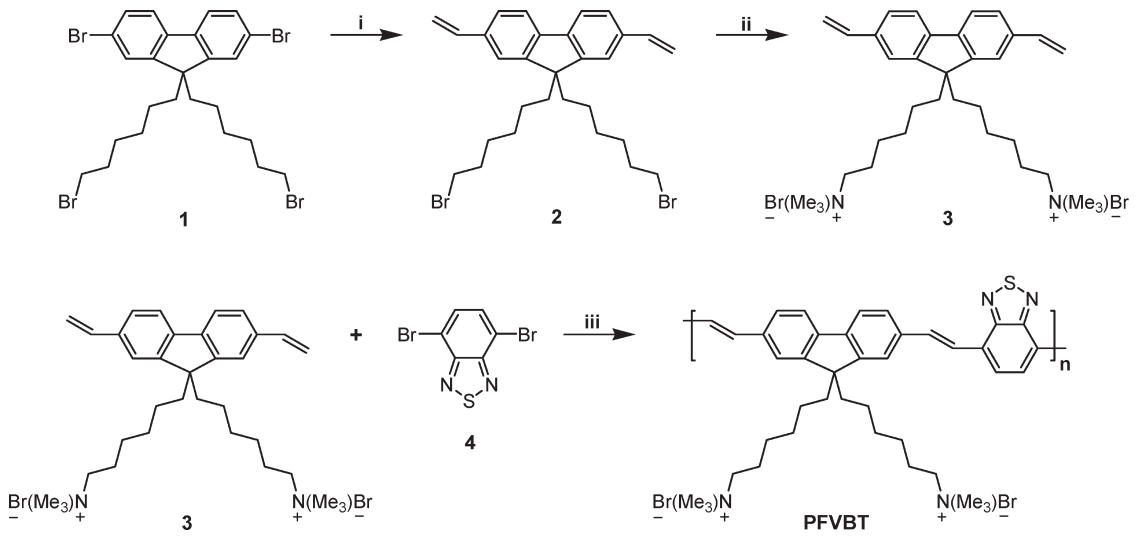

[a] Conditions: (i) tributylvinyltin, $PdCl_2(PPh_3)_2$/2,6-di-*tert*-butylphenol, toluene, 100 °C, 24 h; (ii) trimethylamine, THF/H_2O, −78 °C, 24 h; (iii) $Pd(OAc)_2$/P(*o*-tolyl)$_3$, DMF/water/TEA, 100 °C, 12 h.

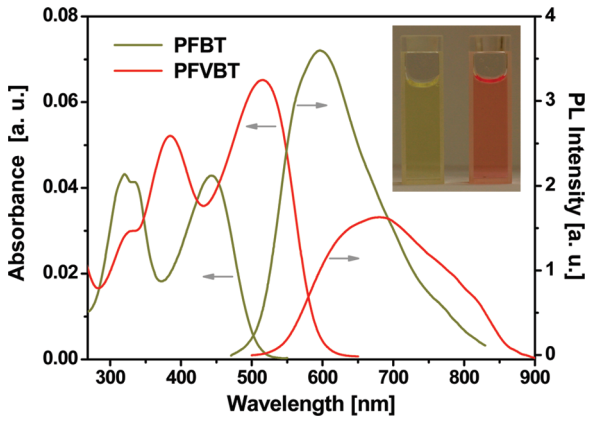

Figure 2. UV−vis absorption and PL spectra of PFBT and PFVBT in aqueous solution at [RU] = 2 μM. Excitation wavelengths for PFBT and PFVBT are 440 and 490 nm, respectively. Inset shows the photographs of the corresponding PFBT (left) and PFVBT (right) solutions.

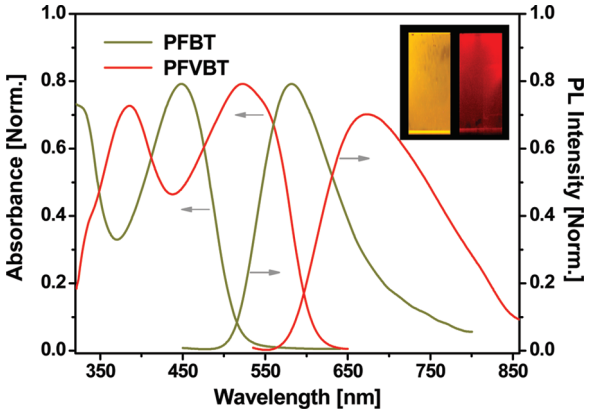

Figure 3. UV−vis absorption and PL spectra of PFBT and PFVBT in thin solid films. Excitation wavelengths for PFBT and PFVBT are 440 and 490 nm, respectively. Inset shows photographs of fluorescent PFBT (left) and PFVBT (right) thin films under UV radiation at 365 nm.

polymer concentrations based on repeat unit (RU) are 2 μM. PFVBT has two absorption maxima at 385 and 515 nm, which correspond to the $\pi-\pi^*$ transitions of the vinyl fluorene segments and the vinyl BT segments, respectively. The absorption maximum of PFVBT is red-shifted by ~70 nm as compared to that of PFBT. The presence of vinyl bonds in the backbone of PFVBT increases the polymer conjugation length, leading to solution color variation from yellow for PFBT to red for PFVBT (the inset in Figure 2). Similarly, the PL maximum of PFVBT in water is at 685 nm, which is red-shifted by 88 nm as compared to that of PFBT (597 nm). The PL quantum yields for PFBT and PFVBT in water are ~0.04 and 0.005, respectively, measured using quinine sulfate in 0.1 M H_2SO_4 (quantum yield = 0.55) as the standard. In addition, the PL quantum yields for PFBT and PFVBT in methanol are ~0.20 and 0.08, respectively, both of which are higher than those in water. The decreased quantum yields of both polymers in water are ascribed to the charge-transfer character of the polymers.[10b]

The solid-state UV−vis absorption and PL spectra of PFBT and PFVBT are depicted in Figure 3. The high-energy absorption maxima in solid state for PFBT and PFVBT are located at 450 and 522 nm, respectively, which are slightly red-shifted by ~5 nm as compared with those in aqueous solution. The bathochromic shift in absorption from the solution to solid state is widely observed for conjugated polymers, which is recognized as a result of the conformation transformation to a more ordered form that facilitates π-electron delocalization along the backbone.[25] The PL maxima of PFBT and PFVBT in solid state are 585 and 675 nm, respectively, which are blue-shifted by ~10 nm in relation to those in aqueous solution. The opposite shifts in the emission and absorption maxima can be rationalized by the charge-transfer character of the polymers, and the blue-shifted emission maxima are caused by decreased environmental polarity upon turning from aqueous solution into solid state. Furthermore, the solid-state PL quantum yields of PFBT and PFVBT are ~0.07 and 0.04, respectively, giving rise to bright fluorescence as shown in the inset of Figure 3. The increased quantum yields and narrowed emission spectra in solid state relative to those in aqueous solutions not only further testify the charge-transfer character of PFBT and PFVBT but also highlight that the polymer fluorescence in aqueous solution can be enhanced through CPE/biomolecule complexation and CPE aggregation.

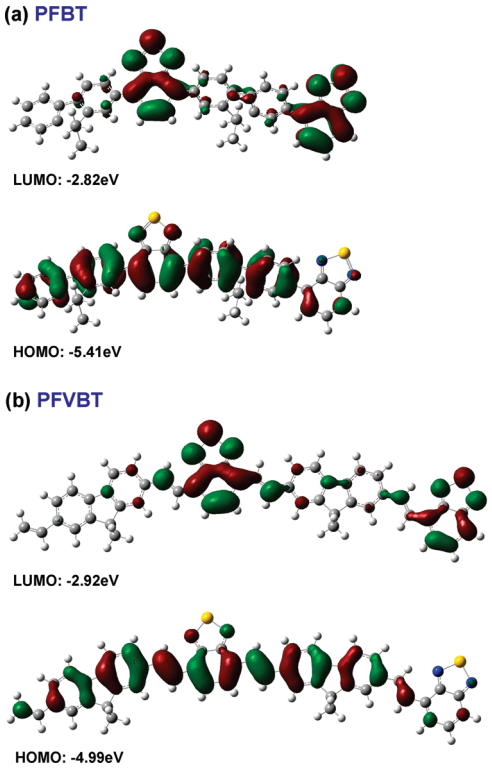

Figure 4. Representation of HOMO and LUMO energy levels and the frontier molecular orbitals of PFBT and PFVBT with a chain length $n = 2$ obtained from DFT calculation at the B3LYP/6-31G* level. The cationic side chains are replaced with methyl groups in the calculations.

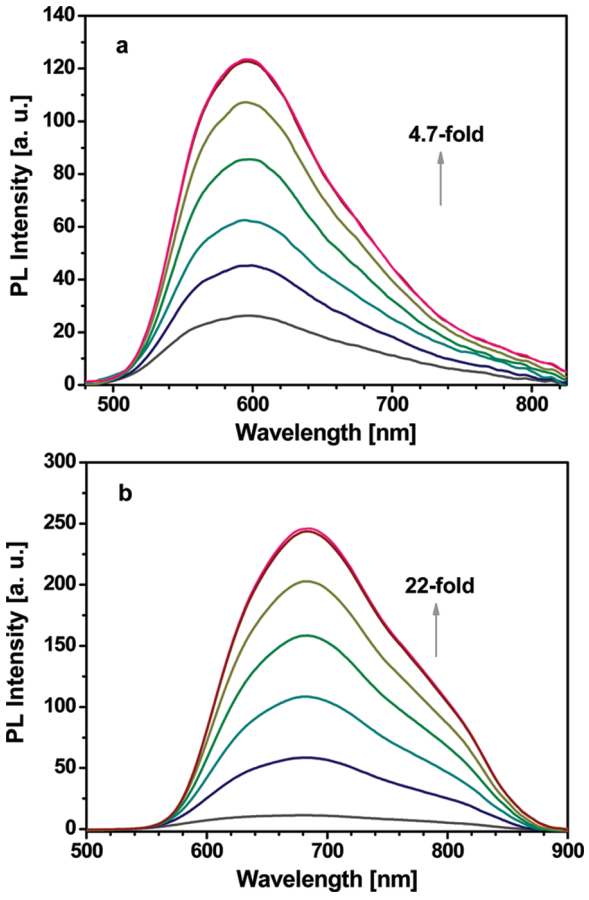

Figure 5. PL spectra of PFBT (a) and PFVBT (b) at [RU] = 10 μM in 2 mM PBS (pH = 7.4) in the presence of DNA with the concentration ranging from 0 to 1.2 μM at intervals of 0.2 μM. Excitation wavelengths for PFBT and PFVBT are 440 and 490 nm, respectively. The arrows indicate the direction of increasing [DNA].

Molecular Orbital Calculations. To understand and compare the charge-transfer electronic states of PFBT and PFVBT from the viewpoint of molecular orbital, density-functional theory (DFT) calculations were conducted for both polymers at the B3LYP/6-31G* level. Figure 4 represents the calculated lowest unoccupied molecular orbital (LUMO) and highest occupied molecular orbital (HOMO) of PFBT and PFVBT with a chain length $n = 2$. Because the side chains at 9-positon of fluorene units are not conjugated with the backbone, they have a weak impact on the energy levels of the fluorene-based molecules.[26] Thereby, the cationic side chains are replaced with methyl groups to simplify the calculation. As shown in Figure 4, the HOMO energy levels for both dimers are nearly delocalized over the π-conjugated systems, while the LUMO energy levels are predominantly localized on the BT units. These results implicate that the HOMO−LUMO transition for PFBT and PFVBT is accompanied by charge transfer from the fluorene segments to the BT units due to the strong electron deficiency of BT units, which are consistent with the previous reports concerning the electronic structure calculations on BT-based polymers.[27]

The DFT calculations also demonstrate that the presence of vinyl bonds lowers HOMO but rises LUMO, together resulting in a smaller energy band gap for PFVBT relative to that of PFBT (Figure 4). Moreover, the dihedral angle between the fluorene plane and the BT plane is ~35° and 0° for PFBT and PFVBT, respectively. According to these data, the charge redistribution upon excitation of PFVBT should be more obvious than that for PFBT. This theoretical speculation is experimentally witnessed by the significantly red-shifted absorption maxima and increased Stokes shift of PFVBT with respect to those of PFBT (Figures 2 and 3). Additionally, the lower PL quantum yield of PFVBT relative to that of PFBT in aqueous solution agrees with the enhanced intramolecular charge transfer by introducing the vinyl bonds. On the basis of these data, PFVBT should have a more sensitive fluorescence response toward environmental variations than PFBT does, which is desirable for chemical and biological sensing.

Multicolor Light-Up Responses toward Biomolecules. The fluorescence responses of PFBT and PFVBT toward DNA and BSA are studied and compared in 2 mM phosphate buffered saline (PBS, pH = 7.4) at [RU] = 10 μM. The DNA concentration is based on strands. As shown in Figure 5, both PFBT and PFVBT exhibit gradually enhanced fluorescence with increasing [DNA]. The analyte saturation occurs at [DNA] = 1.0 μM for both polymers. Since DNA has 20 negative charges per strand, and each polymer repeat unit has 2 positive charges, the concentrations for the positive and negative charges are the same (20 μM) at the saturation point. This indicates that the analyte saturation stems from the charge balance between the oppositely charged polymer and the analyte, which is generally observed for CPE-based sensors with electrostatic attraction as the main driving force.[7b] At [DNA] = 1.0 μM, the fluorescence intensities of PFBT and PFVBT are increased by 4.7-fold, and 22-fold, respectively, as compared to their initial intensities in the absence of DNA. The emission maxima for PFBT/DNA and PFVBT/DNA remain the same as those in the absence of DNA, which are 597 and 685 nm, respectively.

The PL spectra of PFBT and PFVBT in the absence and presence of BSA with [BSA] ranging from 0 to 1.4 μM are

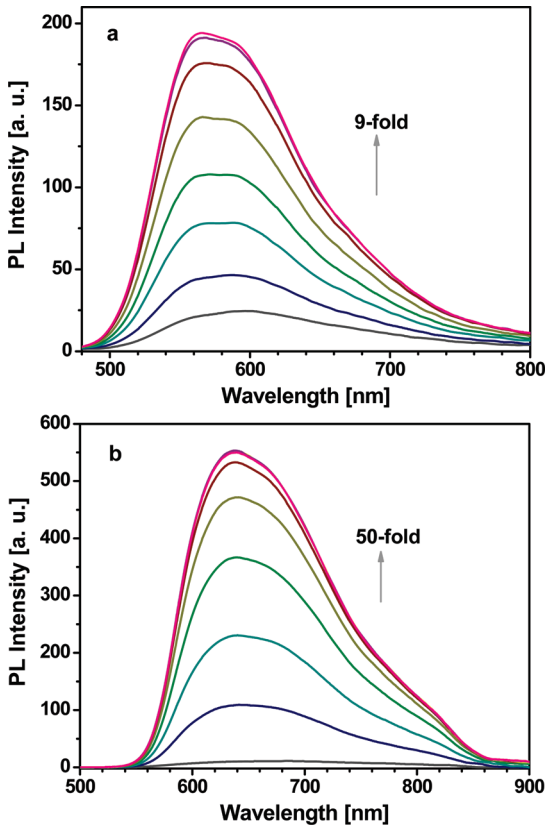

Figure 6. PL spectra of PFBT (a) and PFVBT (b) at [RU] = 10 μM in 2 mM PBS (pH = 7.4) in the presence of BSA with the concentration ranging from 0 to 1.4 μM at intervals of 0.2 μM. Excitation wavelengths for PFBT and PFVBT are 440 and 490 nm, respectively. The arrows indicate the direction of increasing [BSA].

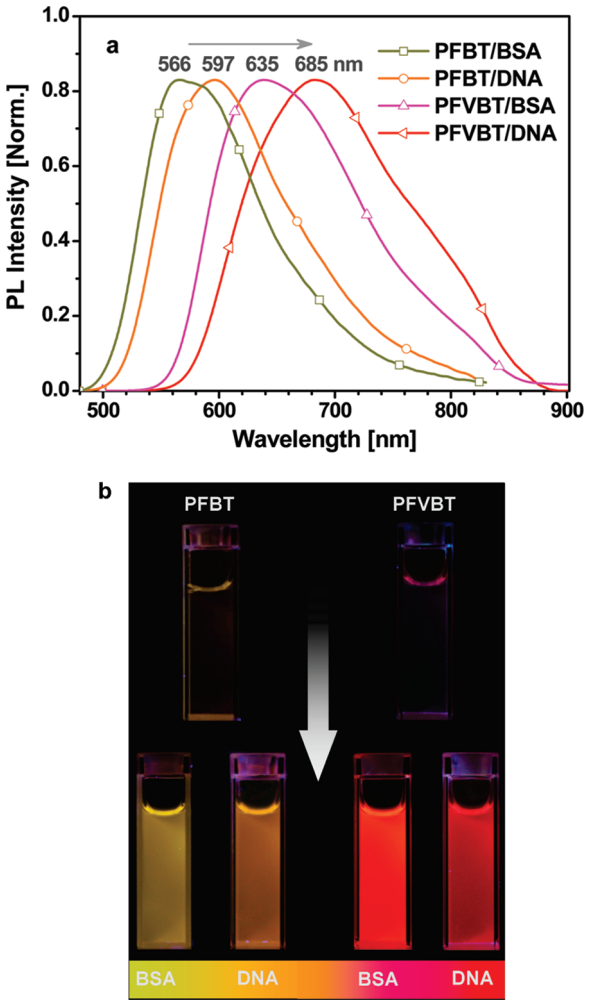

Figure 7. (a) Normalized PL spectra of PFBT and PFVBT at [RU] = 10 μM in 2 mM PBS (pH = 7.4) in the presence of BSA or DNA with the concentration of 1.2 μM. Excitation wavelengths for PFBT and PFVBT are 440 and 490 nm, respectively. (b) Photographs of the corresponding fluorescent polymer solutions in the absence (up) and presence (bottom) of DNA or BSA with the concentration of 1.2 μM under UV radiation at 365 nm. [RU] = 10 μM in 2 mM PBS (pH = 7.4).[31]

displayed in Figure 6. Both polymers show fluorescence intensity increases upon BSA addition, concomitant with the blue-shifted PL maxima. The saturation happens at [BSA] = 1.2 μM for both polymers. Considering that the net charges of BSA are around −17 at pH = 7.4,[28] the saturation conditions are consistent with the charge balance principle as aforementioned. At [BSA] = 1.2 μM, the fluorescence of PFBT and PFVBT increases by 9-fold and 50-fold, respectively, relative to those in the absence of BSA, while the PL maxima of PFBT/BSA and PFVBT/BSA are blue-shifted from 586 and 685 nm in the absence of BSA to 566 and 635 nm, respectively.

These data demonstrate that both DNA and BSA can induce fluorescence enhancement of PFBT and PFVBT in aqueous solution. Noteworthy is that in the previous reports addition of DNA into the aqueous solution of traditional cationic CPEs results in strong fluorescence quenching owing to complexation-induced polymer aggregation.[12b,21b,29] For PFBT and PFVBT, the complex formation between oppositely charged polymers and biomolecules creates a hydrophobic microenvironment to reduce the intensive contact between the electronic backbones of the polymer and water molecules, leading to the light-up responses. In addition, the extent of complexation-enhanced fluorescence of PFBT and PFVBT for BSA is much larger than that for DNA (Figure 6 vs Figure 5), and the emission maxima of both polymers in the presence of BSA are blue-shifted as compared to those in the presence of DNA at the saturation point. These spectral discrepancies indicate that the polymer light-up responses are partially dependent on the analyte. Since BSA is an amphiphilic macromolecule, it has surfactant-like nature in aqueous solution, while DNA is constituted by sugar backbone and phosphate side groups and thus is less amphiphilic. In addition, BSA has hydrophobic pockets in the native folding structure of its chains.[30] As a consequence, BSA provides a more hydrophobic environment for the polymers than DNA does, eventually leading to the larger light-up extent and blue-shifted emission maxima.

To further compare the light-up properties between PFBT and PFVBT, the PL spectra in the presence of DNA or BSA at the saturation points are normalized and presented in Figure 7a. The full width at half-maximum (FWTH) for PFBT in the presence of DNA and BSA are 135 and 115 nm, respectively, while the FWTH for PFVBT in the presence of DNA and BSA are 175 and 148 nm, respectively. Furthermore, the emission maxima for PFBT and PFVBT in the presence of BSA are blue-shifted by 31 and 50 nm, respectively, relative to those in the presence of DNA. These spectral differences indicate that PFVBT has a more sensitive light-up response toward environmental variation than PFBT does. These data are in line with the results drawn from molecular orbital simulations. On the other hand, the light-up color for each polymer is different in the presence of

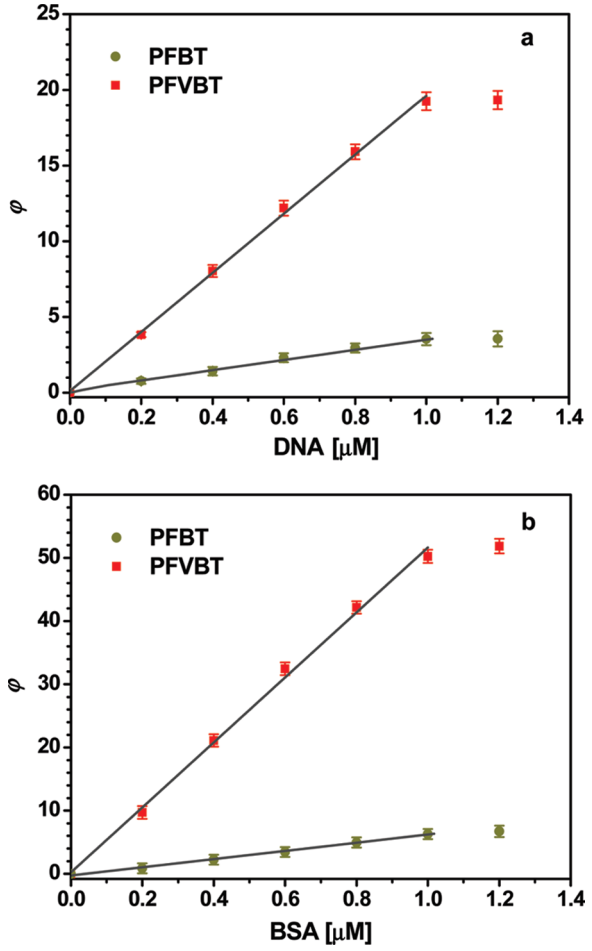

Figure 8. φ as a function of [DNA] (a) or [BSA] (b) and its trendline. The data are based on the average of three independent experiments.

DNA and BSA, as a result of the discrepancies in the emission maxima and FWTH. As depicted in Figure 7b, PFBT emits light yellow and golden fluorescence in the presence of BSA and DNA, respectively, whereas PFVBT emits orange and red fluorescence in the presence of BSA and DNA, respectively. These images provide clear evidence that both PFBT and PFVBT are multicolor light-up probes.

Biomolecular Quantification. To demonstrate and compare the capability of PFBT and PFVBT in biomolecular quantification, the intensity increases in the PL spectra of both polymers upon addition DNA or BSA are correlated with analyte concentrations. The calibration parameter φ is defined as the ratio of the increment in the PL intensity at the emission maximum in the presence of DNA or BSA ($I_{DNA} - I_0$) to that in the absence of DNA or BSA (I_0). This parameter considers the fluorescence background along with the extent of fluorescence enhancement, allowing estimation of the sensitivity of the light-up probes according to the slope of the calibration curve. Figure 8 depicts φ as a function of [DNA] or [BSA] for PFBT and PFVBT together with their trendlines. The good overlap between the trendlines and the original points in the range of 0−1.0 μM verifies the validity of DNA and BSA quantification using these light-up probes. The deviation from the trendline above the DNA or BSA concentration of 1.0 μM is caused by the analyte saturation as aforementioned. The slopes of the calibration curves of DNA are ~3.5 and 19 μM^{-1} for PFBT and PFVBT, respectively, while the slopes of the calibration curves of BSA are ~6.5 and 51 μM^{-1} for PFBT and PFVBT, respectively. The larger slopes of DNA and BSA calibration curves for PFVBT relative to those for PFBT reflect the higher sensitivity of PFVBT, which is beneficial to biological quantification. On the other hand, it is noteworthy that the calibration range can be expanded by using different polymer concentrations as described in our previous report.[15]

Conclusions

In summary, two multicolor CPE-based light-up probes capable of emitting biomolecule-dependent yellow-to-golden and orange-to-red light have been designed for biomolecular quantification. Different from the postpolymerization method used for PFBT, a new facile one-pot Heck-coupling polymerization in aqueous-containing media is adopted to synthesize PFVBT. The high electron-deficiency of BT units endues PFBT and PFVBT with charge-transfer electronic states as witnessed by their solvent-dependent optical properties and molecular orbital simulations, eventually leading to microenvironment-sensitive fluorescence for both polymers. The introduction of vinyl bonds to the conjugated backbone not only imparts larger Stoke shift (170 nm) and longer wavelength emission (685 nm) in aqueous media but also induces a stronger charge-transfer character for PFVBT relative to that of PFBT. The weak fluorescence of both polymers in aqueous solution can be substantially enhanced upon complexation with biomolecules which increases the hydrophobicity of polymeric microenvironment. Upon changing from DNA to BSA, both PFBT and PFVBT show increased fluorescence turn-on responses and blue-shifted emission maxima, resulting in biomolecule-dependent light-up signatures. In comparison with PFBT, PFVBT has a more sensitive light-up response, leading to a higher effectiveness in biomolecular quantification. These findings highlight that the light-up response of charge-transfer based CPEs is strongly correlated to the extent of charge transfer that can be adjusted by backbone modification. Although PFBT and PFVBT are more appropriate for biomolecular quantification than for biomolecular detection, attachment of recognition elements to the polymer side chains could bring in good selectivity. In virtue of their sharp light-up contrast, large Stokes shift, long-wavelength emission, linear calibration curve, and sufficient water solubility, charge-transfer based CPEs provide an intriguing platform for chemical and biological sensing.

Experimental Section

Instruments. NMR spectra were collected on Bruker Avance 500 (DRX 500, 500 MHz). Matrix-assisted laser desorption/ionization time-of-flight (MALDI-TOF) was performed by using 2,5-dihydroxybenzoic acid (DHB) as the matrix under the reflector mode for data acquisition. Element analysis was performed on Perkin-Elmer 2400 CHN/CHNS and Eurovector EA3000 elemental analyzers. UV−vis absorption spectra were recorded on a Shimadzu UV-1700 spectrometer. PL measurements were carried out on a Perkin-Elmer LS-55 equipped with a xenon lamp excitation source and a Hamamatsu (Japan) 928 PMT, using 90° angle detection for solution samples. The excitation energy at different wavelength was automatically adjusted to the same level by an excitation correction file. PL quantum yields were measured using quinine sulfate as the standard, with a quantum yield of 55% in H_2SO_4 (0.1 M). Millex syringe driven filters (0.22 μm, PVDF) were used to exclude the insoluble substances in the polymer solution before dialysis process. Fisher brand regenerated cellulose dialysis tubing with 6.5 kDa molecular weight cutoff was used for polymer dialysis. Freeze-drying was performed using Martin Christ Model Alpha 1-2/LD. Photographs of the polymer solutions and thin films were taken using a Canon EOS 400D

digital camera under a hand-held UV-lamp with $\lambda_{max} = 365$ nm. The polymer thin films for UV−vis absorption and PL experiments were prepared by spin-coating from polymer solution (5 mg/mL) onto the quartz plates. All PL and UV measurements were carried out at 24 ± 1 °C. The quantum-chemical calculations of the polymers with $n = 2$ were performed using the Gaussian 03 software package. Ground-state geometries were optimized at the Becke's three-parameter hybrid functional using the Lee−Yang−Parr correlation functional (B3LYP) level with the 6-31G* basis set. Vibrational analysis was carried at the same levels of the theory to optimize the structure as equilibrium structures.

Materials. HPLC-purified DNA oligonucleotide (5′-ATC TTG ACT ATG TGG GTG CT-3′) was purchased from Research Biolabs, Singapore. 10 × PBS buffer with pH = 7.4 (ultrapure grade) is a commercial product of first BASE Singapore. Milli-Q water (18.2 MΩ) was used to prepare the buffer solutions from the 10 × PBS stock buffer. 1 × PBS contains NaCl (137 mM), KCl (2.7 mM), Na_2HPO_4 (10 mM), and KH_2PO_4 (1.8 mM). Fresh stock solutions for PFBT (1 mM), PFVBT (1 mM), BSA (1 mM), (1 mM), and ssDNA (0.1 mM) were prepared before use. NMR solvents, D_3-chloroform (99%) and D_4-methanol (99.5%), were purchased from Cambridge Isotope Laboratories, Inc. 2,7-Dibromo-9,9-bis(6′-bromohexyl)fluorene (**1**), 4,7-dibromobenzothiadiazole (**4**), and poly[9,9-bis(6′-*N*,*N*,*N*-trimethylammonium)hexyl)fluorene-*alt*-4,7-(2,1,-3-benzothiadiazole) dibromide] (PFBT) were synthesized according to our previous report.[21] The number-average DP of PFBT is ∼16. Other chemicals and biological reagents were purchased from Sigma-Aldrich Chemical Co. and were used as received.

Synthesis of 9,9-Bis(6′-bromohexyl)-2,7-divinylfluorene (2). 2,7-Dibromo-9,9-bis(6-bromohexyl)-fluorene (**1**) (1.30 g, 2.0 mmol), tributylvinyltin (1.33 g, 4.2 mmol), $PdCl_2(PPh_3)_2$ (56 mg, 0.09 mmol), 2,6-di-*tert*-butylphenol (8 mg, 38 mmol), and toluene (20 mL) were mixed in a 50 mL flask. The reaction mixture was stirred and heated at 100 °C for 24 h under N_2. After cooling to the room temperature, the mixture was diluted with ether and treated with KF solution (∼10%), which was followed by stirring for 12 h. The mixture was then filtrated to remove the insoluble solid, and the filtrate was dried over anhydrous Na_2SO_4. The solvent was removed under reduced pressure, and the residue was purified by silica gel chromatograph using hexane/dichloromethane (5:1) as eluent to give **2** (0.85 g, 78%) as white crystals. ^{1}H NMR (500 MHz, $CDCl_3$, δ ppm): 7.62 (d, 2 H, J = 7.83 Hz), 7.40 (d, 2 H, J = 7.85 Hz), 7.35 (s, 2 H), 6.80 (dd, 2 H, J = 10.86, 17.58), 5.81 (d, 2 H, J = 17.58 Hz), 5.27 (2 H, d, J = 10.86), 3.27 (t, 4 H, J = 6.81, 6.81), 1.97 (m, 4 H), 1.65 (q, 4 H), 1.19 (q, 4 H), 1.07 (q, 4 H), 0.63 (m, 4 H). ^{13}C NMR (125 MHz, $CDCl_3$, δ ppm): 151.38, 141.39, 137.71, 136.99, 125.81, 120.78, 120.19, 113.58, 55.21, 40.65, 34.35, 33.03, 29.43, 28.13, 23.86. Element analysis calcd (%) for $C_{29}H_{36}Br_2$: C 63.98 H 6.67. Found: C 64.18, H 6.63. MS (MALDI-TOF): m/z 544.51 $[M]^+$.

Synthesis of 9,9-Bis(6′-(*N*,*N*,*N*,-trimethylammonium)hexyl)-2,7-divinylfluorene Dibromide (3). Condensed trimethylamine (∼3 mL) was added dropwise to a solution of **2** (163 mg, 0.30 mmol) in THF (5 mL) at −78 °C. The mixture was allowed to warm to room temperature. The precipitate was redissolved by adding H_2O (5 mL). After the mixture was cooled to −78 °C, additional trimethylamine (∼3 mL) was added. The mixture was stirred at room temperature for 24 h. After removal of the solvent, acetone was added to precipitate **3** (188 mg, 95%) as white powders. ^{1}H NMR (500 MHz, CD_3OD, δ ppm): 7.94 (d, 2H, J = 7.83), 7.76 (s, 2 H), 7.69 (d, 2 H, J = 9.14), 7.08 (dd, 2 H, J = 10.93, 17.63), 6.61 (d, 2 H, J = 17.63), 5.51 (d, 2 H, J = 10.93), 3.46−3.40 (m, 4 H), 3.29 (s, 18 H), 2.42−2.26 (m, 4 H), 1.93−1.73 (m, 4 H), 1.52−1.35 (m, 8 H), 0.92−0.78 (m, 4 H). ^{13}C NMR (125 MHz, CD_3OD, δ ppm): 152.28, 142.27, 138.52, 138.27, 126.63, 121.55, 120.89, 113.72, 67.67, 56.14, 53.52, 41.01, 29.96, 26.63, 24.47, 23.41. MS (MALDI-TOF): m/z 581.61 $[M - Br]^+$.

Synthesis of Poly[9,9-bis(6′-(*N*,*N*,*N*-trimethylammonium)-hexyl)fluorenyldivinylene-*alt*-4,7-(2,1,3-benzothiadiazole) Dibromide] (PFVBT). A Schlenk tube was charged with **3** (140 mg, 0.212 mmol), **4** (62 mg, 0.212 mmol), $Pd(OAc)_2$ (2 mg, 9 μmmol), and P(*o*-tolyl)$_3$ (15 mg, 49 μmol) before it was sealed with a rubber septum. The Schlenk tube was degassed with three vacuum−argon cycles to remove air. Then, DMF (1 mL), H_2O (0.5 mL), and triethylamine (1 mL) were added to the Schlenk tube, and the mixture was frozen, evacuated, and thawed three times to further remove air. The polymerization was carried out at 100 °C under vigorous stir for 12 h. It was then filtered through 0.22 μm syringe driven filter, and the filtrate was poured into acetone. The precipitate was collected and redissolved in methanol. Finally, the polymer was purified by dialysis against Mill-Q water using a 6.5 kDa molecular weight cutoff dialysis membrane for 5 days. After freeze-drying, PFVBT (138 mg, 82%) was obtained as red fibers. ^{1}H NMR (500 MHz, CD_3OD, δ ppm): 8.75−7.05 (m, 12 H), 6.91 (br, ∼0.25 H) 5.95 (br, ∼0.25 H), 5.35 (br, ∼0.25 H), 3.25 (br, 4 H), 3.07 (br, 18 H), 2.25 (br, 4 H), 1.60 (br, 4 H), 1.21 (br, 8 H), 0.80 (br, 4 H). ^{13}C NMR (125 MHz, CD_3OD, δ ppm): 155.23, 153.23, 142.21, 138.58, 135.10, 130.53, 128.78, 127.45, 125.42, 120.40, 67.69, 56.42, 53.62, 41.13, 30.12, 26.73, 24.88, 23.58.

Acknowledgment. The authors are grateful to the National University of Singapore (ARF R-279-000-234-123) and Singapore Ministry of Education (R-279-000-255-112) for financial support. The authors also thank Mr. Yutao Liu for photographing.

References and Notes

(1) (a) Piunno, P. A. E.; Krull, U. J. *Anal. Bioanal. Chem.* **2005**, *381*, 1004–1011. (b) Borisov, S. M.; Wolfbeis, O. S. *Chem. Rev.* **2008**, *108*, 423–461.

(2) (a) Zhang, J.; Campbell, R. E.; Ting, A. Y.; Tsien, R. Y. *Nat. Rev. Mol. Cell Biol.* **2002**, *3*, 906–918. (b) Marti, A. A.; Jockusch, S.; Stevens, N.; Ju, J.; Turro, N. J. *Acc. Chem. Res.* **2007**, *40*, 402–409. (c) Cravatt, B. F.; Wright, A. T.; Kozarich, J. W. *Annu. Rev. Biochem.* **2008**, *77*, 383–414.

(3) (a) Lim, M. H.; Xu, D.; Lippard, S. J. *Nat. Chem. Biol.* **2006**, *2*, 375–380. (b) Lim, M. H.; Lippard, S. J. *Acc. Chem. Res.* **2007**, *40*, 41–51. (c) Domaille, D. W.; Que, E. L.; Chang, C. J. *Nat. Chem. Biol.* **2008**, *4*, 168–175.

(4) (a) Haugland, R. P. *Handbook of Fluorescent Probes and Research Chemicals*; Molecular Probes: Leiden, 2002. (b) Royer, C. A. *Chem. Rev.* **2006**, *106*, 1769–1784.

(5) (a) Tong, H.; Hong, Y.; Dong, Y.; Haussler, M.; Lam, J. W. Y.; Li, Z.; Guo, Z.; Guo, Z.; Tang, B. Z. *Chem. Commun.* **2006**, 3705–3707. (b) Tong, H.; Hong, Y.; Dong, Y.; Haussler, M.; Li, Z.; Lam, J. W. Y.; Dong, Y.; Sung, H. H. Y.; Williams, I. D.; Tang, B. Z. *J. Phys. Chem. B* **2007**, *111*, 11817–11823. (c) Wang, M.; Zhang, D.; Zhang, G.; Tang, Y.; Wang, S.; Zhu, D. *Anal. Chem.* **2008**, *80*, 6443–6448. (d) Li, Z.; Dong, Y. Q.; Lam, J. W. Y.; Sun, J.; Qin, A.; Haussler, M.; Dong, Y. P.; Sung, H. H. Y.; Williams, I. D.; Kwok, S. H.; Tang, B. Z. *Adv. Funct. Mater.* **2009**, *19*, 905–917.

(6) (a) Thomas, S. W.III; Joly, G. D.; Swager, T. M. *Chem. Rev.* **2007**, *107*, 1339–1380. (b) Herland, A.; Inganas, O. *Macromol. Rapid Commun.* **2007**, *28*, 1703–1713. (c) Nilsson, K. P. R.; Hammarström, P. *Adv. Mater.* **2008**, *20*, 2639–2645. (d) Ho, H. A.; Najari, A.; Leclerc, M. *Acc. Chem. Res.* **2008**, *41*, 168–178.

(7) (a) Swager, T. M. *Acc. Chem. Res.* **1998**, *31*, 201–207. (b) Pu, K. Y.; Liu, B. *Biosens. Bioelectron.* **2009**, *24*, 1067–1073.

(8) (a) Chen, L.; McBranch, D. W.; Wang, H. L.; Helgeson, R.; Wudl, F.; Whitten, D. G. *Proc. Natl. Acad. Sci. U.S.A.* **1999**, *96*, 12287–12292. (b) Wang, D.; Gong, X.; Heeger, P. S.; Rininsland, F.; Bazan, G. C.; Heeger, A. J. *Proc. Natl. Acad. Sci. U.S.A.* **2002**, *109*, 49–53. (c) Nilsson, K. P. R.; Rydberg, J.; Baltzer, L.; Inganas, O. *Proc. Natl. Acad. Sci. U.S.A.* **2003**, *110*, 10170–10174. (d) Pinto, M. R.; Schanze, K. S. *Proc. Natl. Acad. Sci. U.S.A.* **2004**, *101*, 7505–7510. (d) Ho, H. A.; Leclerc, M. *J. Am. Chem. Soc.* **2004**, *126*, 1384–1387. (e) (f) Lee, K.; Cho, J. C.; DeHeck, J.; Kim, J. *Chem. Commun.* **2006**, 1983–1985.

(f) Miranda, O. R.; You, C. C.; Phillips, R.; Kim, I. B.; Ghosh, P. S.; Bunz, U. H. F.; Rotello, V. M. *J. Am. Chem. Soc.* **2007**, *129*, 9856–9857.
(9) (a) McQuade, D. T.; Hegedus, A. H.; Swager, T. M. *J. Am. Chem. Soc.* **2002**, *122*, 12389–12390. (b) Gaylord, B. S.; Heeger, A. J.; Bazan, G. C. *Proc. Natl. Acad. Sci. U.S.A.* **2002**, *99*, 10954–10957. (c) Ho, H. A.; Doŕe, K.; Boissinot, M.; Bergeron, M. G.; Tanguay, R. M.; Boudreau, D.; Leclerc, M. *J. Am. Chem. Soc.* **2005**, *127*, 12673–12676. (d) Liu, B.; Bazan, G. C. *Chem. Mater.* **2004**, *16*, 4467–4476. (e) He, F.; Tang, Y.; Wang, S.; Li, Y.; Zhu, D. *J. Am. Chem. Soc.* **2005**, *127*, 12343–12346. (f) Lee, K.; Rouillard, J.-M.; Pham, T.; Gulari, E.; Kim, J. *Angew. Chem., Int. Ed.* **2007**, *46*, 4667–4670. (g) Lee, K.; Maisel, K.; Rouillard, J. M.; Gulari, E.; Kim, J. *Chem. Mater.* **2008**, *20*, 2848–2850.
(10) (a) Zhao, X. Y.; Liu, Y.; Schanze, K. S. *Chem. Commun.* **2007**, 2914–2916. (b) Pu, K. Y.; Liu, B. *Adv. Funct. Mater.* **2009**, *19*, 277–284. (c) Lee, K.; Povlich, L. K.; Kim, J. *Adv. Funct. Mater.* **2007**, *17*, 2580–2587.
(11) (a) Liu, B.; Gaylord, B. S.; Wang, S.; Bazan, G. C. *J. Am. Chem. Soc.* **2003**, *125*, 6705–6714. (b) Xu, Q. H.; Gaylord, B. S.; Wang, S.; Bazan, G. C.; Moses, D.; Heeger, A. J. *Proc. Natl. Acad. Sci. U.S.A.* **2004**, *101*, 11634–11639.
(12) (a) Li, C.; Numata, M.; Takeuchi, M.; Shinkai, S. *Angew. Chem., Int. Ed.* **2005**, *44*, 6371–6374. (b) Pu, K. Y.; Pan, S. Y. H.; Liu, B. *J. Phys. Chem. B* **2008**, *112*, 9295–9300.
(13) (a) Hong, J. W.; Hemme, W. L.; Keller, G. E.; Rinke, M. T.; Bazan, G. C. *Adv. Mater.* **2006**, *18*, 878–882. (b) Chi, C.; Mikhailovsky, A.; Bazan, G. C. *J. Am. Chem. Soc.* **2007**, *129*, 11134–11145.
(14) Liu, B.; Bazan, G. C. *J. Am. Chem. Soc.* **2004**, *126*, 1942–1943.
(15) Pu, K. Y.; Liu, B. *Macromolecules* **2008**, *41*, 6636–6640.
(16) Yu, D.; Zhang, Y.; Liu, B. *Macromolecules* **2008**, *41*, 4003–4011.
(17) Pu, K. Y.; Liu, B. *Adv. Funct. Mater.* **2009**, *19*, 1371–1378.
(18) Lakowicz, J. R. *Principles of Fluorescence Spectroscopy*, 3rd ed.; Springer Science R Business Media, LLC: New York, 2006.
(19) Nelson, D. L.; Cox, M. M. *Lehninger Principles of Biochemistry*, 4th ed.; W.H. Freeman: New York, 2004.
(20) Li, C.; Numata, M.; Bae, A. H.; Sakurai, K.; Shinkai, S. *J. Am. Chem. Soc.* **2005**, *127*, 4548–4549.
(21) (a) Liu, B.; Bazan, G. C. *Nat. Protoc.* **2006**, *1*, 1698–1702. (b) Pu, K. Y.; Fang, Z.; Liu, B. *Adv. Funct. Mater.* **2008**, *18*, 1321–1328.
(22) Liao, L.; Pang, Y.; Ding, L. M.; Karasz, F. E. *Macromolecules* **2001**, *34*, 7300–7305.
(23) (a) Mikroyannidis, J. A.; Barberis, V. P. *J. Polym. Sci., Part A: Polym. Chem.* **2007**, *45*, 1481–1491. (b) Grisorio, R.; Piliego, C.; Striccoli, M.; Cosma, P.; Fini, P.; Gigli, G.; Mastrorilli, P.; Suranna, G. P.; Nobile, C. F. *J. Phys. Chem. C* **2008**, *112*, 20076–20087.
(24) Kwasniewski, S. P.; François, J. P.; Deleuze, M. S. *J. Phys. Chem. A* **2003**, *107*, 5168–5180.
(25) Schwartz, B. J. *Annu. Rev. Phys. Chem.* **2003**, *54*, 141–172.
(26) Cornil, J.; Gueli, I.; Dkhissi, A.; Sancho-Garcia, J. C.; Hennebicq, E.; Calbert, J. P.; Lemaur, V.; Beljonne, D.; Brédas, J. L. *J. Chem. Phys.* **2003**, *118*, 6615–6623.
(27) Fratiloiu, S.; Fonseca, S. M.; Grozema, F. C.; Burrows, H. D.; Costa, M. L.; Charas, A.; Morgado, J.; Siebbeles, L. D. A. *J. Phys. Chem. C* **2007**, *111*, 5812–5820.
(28) Peters, T. J. *Adv. Protein Chem.* **1985**, *37*, 161–245.
(29) (a) Nakao, H.; Hayashi, H.; Iwata, F.; Karasawa, H.; Hirano, K.; Sugiyama, S.; Ohtani, T. *Langmuir* **2005**, *21*, 7945–7950. (b) Liu, B.; Bazan, G. C. *J. Am. Chem. Soc.* **2006**, *128*, 1188–1196. (c) Attar, H. A. A.; Monkman, A. P. *J. Phys. Chem. B* **2007**, *111*, 12418–12426. (e) Pu, K. Y.; Zhan, R.; Liu, B. *Macromol. Symp.* **2009**, *279*, 48–51.
(30) Gold, M. G.; Barford, D.; Komander, D. *Curr. Opin. Struct. Biol.* **2006**, *16*, 693–707.
(31) UV light disturbs the real fluorescence color of the polymer solutions in the absence of biomolecules because the fluorescence is very weak.